Vol. 1(2), pp. 1-8, December 2022
DOI: 10.0001/AJPC2021.0207
ISSN 2021-xxxx

ASEAN Journal of Process Control

Research Article

MSC-RS Design Algorithm of PIDF Controller using SOPDT Model

Jameson Malang, Jobrun Nandong, Wan Sieng Yeo

Department of Chemical and Energy Engineering, Curtin University Malaysia, 98009 Miri, Sarawak, MALAYSIA

*Corresponding Author: jameson@curtin.edu.my

Academic Editor: Haslinda Zabiri
Received: 01 November 2022; Accepted: 30 November 2022; Published: 01 December 2022

Abstract: For many decades the process industry has relied on PID control to boost plant performance and safety despite the availability of several advanced control techniques. Crucial to realising the benefits of PID control is finding the tuning values, which is challenging because a plant usually requires many control loops. Poor PID control tuning often becomes one of the reasons why a process plant performs below expectations. Many PID tuning rules are available, some of which have become well-accepted in the industry. The current paper presents a new tuning rule for designing a PID controller augmented with a filter based on combining the multi-scale control scheme and Routh stability criteria (MSC-RS design algorithm). Applying the algorithm to the Coal Mill temperature control demonstrates the effectiveness of the new rule compared to some of the well-known PID tuning methods adopted in the industry.

Keywords: PID Control, SOPDT Model, AMIGO, Routh Stability, Multi-Scale Control.

1. Introduction

The Proportional-Integral-Derivative (PID) control makes up about 80% of the industrial controllers in the process industry [1]. Several advanced control techniques are available such as Model Predictive Control (MPC), but their applications are far less widespread than the PID technique. Such applications of the PID technique are due to several factors, among which its simplicity and robustness are the most cited advantages over advanced control techniques.

Good PID tuning is vital to boost plant performance. Unfortunately, many industrial PID controllers have poor tunings, which caused the plants involved to perform below expectations [2]. The Ziegler-Nichols (ZN) method established several decades ago (in 1940s) has provided a systematic approach to tuning PID controllers in the process industry. However, the performance of the PID controller obtained using the ZN method is sometimes unpredictable, i.e., either sluggish performance or highly oscillatory. Today, many tuning rules are available for PI/PID controller tuning. Numerous existing tuning rules are accessible in a handbook [3]. For more information, interested readers may refer to a recent review of PID tuning methods and applications [4].

Although several more recent tuning rules have emerged over the last four decades, which can outperform the classical ZN tuning method, two of the most well-accepted methods in the process industry are the SIMC [5] and AMIGO [6]. Both tuning methods are available in the MATLAB™ Control System Designer (vs. 2015a or later). Note that a designer can design a PID controller via many different theories such as Internal Model Control (IMC), Direct Synthesis, Frequency Response, and many more.

A recent one is the multi-scale control (MSC) scheme which requires the process model decomposition into a few basic modes. This work investigates whether MSC-based PID can provide improved performance over the well-established AMIGO and SIMC. Besides, the MSC scheme allows for a simpler design procedure to be developed based on each of the simple modes [7].

The present work aims to extend the MSC scheme to derive a PID tuning rule based on the second-order model subject to Routh stability criteria. Specifically, the novelty of the present work lies in combining the MSC theory with the stability theorem in [8].

The structure of the remaining parts of this paper is as follows. Section 2 presents the concept of the multi-scale control scheme, derivation of PID controller stability region, and MSC-RS design algorithm. Next, Section 3 provides a case study to demonstrate the applicability of the proposed MSC-RS design algorithm. Finally, Section 4 highlights some concluding remarks and future research directions.

2. Methodology

2.1. Multi-Scale Control Scheme

According to the MSC scheme, a process consists of several modes (or factors), where each one is representable using a first-order or second-order system. The first-order system can represent a mode that behaves monotonically (without oscillation), and the second-order underdamped system to represent a mode exhibiting oscillatory dynamics. Figure 1 shows the block diagram of the MSC scheme where the process is decomposable into two factors: $P = M_1 + M_2$. The arrangement of the modes M_j for $j = 1, 2$ is in the order from slow to fast dynamics. Hence, M_1 has slower dynamics than M_2. For more details about the multi-scale control scheme, interested readers may refer to [7], [9]. Note that G_{c1}, G_{c2}, W_2 and P denote the outer-loop controller, inner-loop controller, multi-scale predictor, and process transfer functions, respectively. Meanwhile, R, E_1, S, E_2, U and Y denote the external setpoint, outer-loop error, internal setpoint, inner-loop error, manipulated variable, and controlled variable signals, respectively. Note that we choose the faster mode to become the multi-scale predictor, i.e., $W_2 = M_2$.

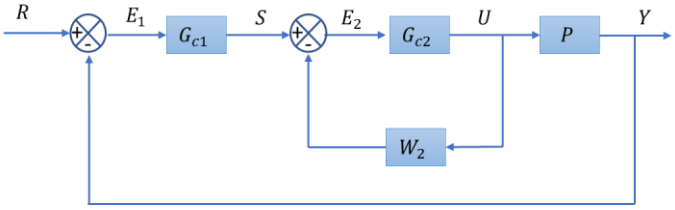

Figure 1. Block diagram of two-layer multi-scale control scheme.

Based on Figure 1, the closed-loop transfer function from S to U is given by,

$$H_I(s) = \frac{G_{c2}(s)}{1 + G_{c2}(s)W_2(s)} \tag{1}$$

The overall closed-loop transfer function from R to Y is as follows:

$$H_r(s) = \frac{G_{c1}(s)P_a(s)}{1 + G_{c1}(s)P_a(s)} \tag{2}$$

where $P_a = H_I P$ represents the augmented process.

The overall multi-scale controller is expressible as below:

$$G_{msc}(s) = G_{c1}(s)H_I(s) \tag{3}$$

Note that when the P-only controller is in the inner loop while the PI controller is in the outer one, the resulting multi-scale controller is transformable into a PID controller [10].

2.2. PIDF Controller Design

To apply the MSC scheme to designing an ideal PID controller augmented with a filter (PIDF controller), let us consider a process model given as follows:

$$G_m(s) = \frac{K_m e^{-\theta_m s}}{(\tau_{m1}s + 1)(\tau_{m2}s + 1)} \quad where \ \tau_{m1} > \tau_{m2} > 0 \tag{4}$$

The process representation above is often well-known as the Second-Order plus Deadtime (SOPDT) model. The decomposition of the model results in the following two modes (M_1 and M_2):

$$G_m(s) = \underbrace{\frac{k_1 e^{-\theta_m s}}{\tau_{m1}s + 1}}_{M_1} + \underbrace{\frac{k_2 e^{-\theta_m s}}{\tau_{m2}s + 1}}_{M_2} \tag{5}$$

where the mode gains are given by,

$$\begin{cases} k_1 = \dfrac{K_m \tau_{m1}}{\tau_{m1} - \tau_{m2}} \\ k_2 = \dfrac{K_m \tau_{m2}}{\tau_{m2} - \tau_{m1}} \end{cases} \tag{6}$$

Assumptions:

- P-only controller for controlling the inner mode M_2.
- PI controller for controlling the outer mode M_1.
- $e^{-\theta_m s} \approx 1 - \theta_m s$ (i.e., first-order Taylor approximation).

The generalised characteristic equation for the inner-layer is given by:

$$(\tau_{m2} - K_{L2}\theta_m)s + K_{L2} + 1 = 0 \tag{7}$$

where K_{L2} denotes the loop gain for the inner loop, i.e., $K_{L2} = K_{c2}K_2$ and K_{c2} is the controller gain.

Applying Routh's necessary stability criterion to the characteristic equation results in the stabilising region for the inner controller given as follows:

$$K_{c2} = \frac{r_{p2}}{k_2}\left(\frac{\tau_{m2}}{\theta_m}\right), \qquad 0 < r_{p2} < 1 \tag{8}$$

The setpoint transfer function corresponding to the inner loop becomes as follows:

$$H_I(s) = \frac{K_{a2}(\tau_{m2}s + 1)}{\tau_{c2}s + 1} \tag{9}$$

where K_{a2} and τ_{c2} are expressible as functions of mode parameters and dimensional parameter:

$$\begin{cases} K_{a2} = \dfrac{r_{p2}\tau_{m2}}{k_2\left(r_{p2}\tau_{m2} + \theta_m\right)} \\ \tau_{c2} = \dfrac{\tau_{m2}\theta_m\left(1 - r_{p2}\right)}{r_{p2}\tau_{m2} + \theta_m} \end{cases} \tag{10}$$

The augmented process model is as follows:

$$P_a(s) = H_I(s)G_m(s) = \frac{K_{a1}e^{-\theta_m s}}{(\tau_{m1}s + 1)(\tau_{c2}s + 1)} \tag{11}$$

where $K_{a1} = K_m K_{a2}$

The closed-loop setpoint transfer function is expressed as follows:

$$H_r(s) = \frac{G_{c1}(s)P_a(s)}{1 + G_{c1}(s)P_a(s)} \tag{12}$$

Note that the PI controller (outer layer sub-controller) is given by,

$$G_{c1}(s) = K_{c1}\left(1 + \frac{1}{\tau_I s}\right) \tag{13}$$

where K_{c1} and τ_I denote the controller gain and reset time, respectively.

The generalised characteristic equation corresponding to the outer layer sub-controller takes the following form:

$$\begin{cases} \tau_{m1}\tau_{c2}\tau_I s^3 + \tau_I(\tau_{m1} + \tau_{c2} - K_{L1}\theta_m)s^2 \ldots \\ \quad +[\tau_I + K_{L1}(\tau_I - \theta_m)]s + K_{L1} = 0 \end{cases} \tag{14}$$

where $K_{L1} = K_{c1}K_{a1}$ denoting the loop gain for the outer loop.

By choosing $\tau_I > \theta_m$ (i.e., a lower limit on the reset time, $\underline{I}_a = \theta_m$), there are one upper limit and two lower limits on the loop gain K_{L1} as below:

$$\begin{cases} K_{L1} < \overline{K}_{L1} = \dfrac{\tau_{m1} + \tau_{c1}}{\theta_m} \\ K_{L1} > \underline{K}_{L1a} = \dfrac{-\tau_I}{\tau_I - \theta_m} \\ K_{L1} > \underline{K}_{L1b} = 0 \end{cases} \tag{15}$$

The stability region for the PI controller is expressible as below:

$$\begin{cases} K_{c1} = \dfrac{r_{p1}}{K_{a1}}\left(\dfrac{\tau_{m1} + \tau_{c2}}{\theta_m}\right) \ \ where\ 0 < r_{p1} < 1 \\ \tau_I = r_i\theta_m \ \ where\ r_i > 1 \end{cases} \tag{16}$$

Note that the stability region above corresponds to Routh's necessary stability criterion. Since Routh's necessary criterion cannot guarantee closed-loop stability, we must adopt the Routh sufficient stability condition to refine the stability region above. In this case, we shall find another limit on the reset time given K_{c1} by the necessary stability criterion. Alternatively, we can find an additional limit for the loop gain where the reset time takes the range following the Routh necessary stability criterion. In this work, we adopt the first approach.

Based on the sufficient stability criterion, one can show that the reset time has another lower limit given by,

$$\tau_I = \underline{I}_b = \frac{K_{L1}}{1+K_{L1}}\left(\theta_m + \frac{\tau_{m1}\tau_{c2}}{\tau_{m1}+\tau_{c2}-K_{l1}\theta_m}\right) \tag{17}$$

Since the reset time has two lower limits, the reset time must be greater than the maximum lower limit to achieve closed-loop stability. Hence, $\tau_I > max(\underline{I}_a, \underline{I}_b)$ and the refined stability region should be as follows:

$$\begin{cases} K_{c1} = \dfrac{r_{p1}}{K_{a1}}\left(\dfrac{\tau_{m1}+\tau_{c2}}{\theta_m}\right) \ \ where\ 0 < r_{p1} < 1 \\ \tau_I = r_i\left[max(\underline{I}_a, \underline{I}_b)\right] \ \ where\ r_i > 1 \\ \underline{I}_a = \theta_m,\ \underline{I}_b = \dfrac{K_{L1}}{1+K_{L1}}\left(\theta_m + \dfrac{\tau_{m1}\tau_{c2}}{\tau_{m1}+\tau_{c2}-K_{l1}\theta_m}\right) \end{cases} \tag{18}$$

Note that the overall multi-scale controller is given as follows:

$$G_{msc}(s) = K_{c1}K_{a2}\left(1+\frac{1}{\tau_I s}\right)\left(\frac{\tau_{m2}s+1}{\tau_{c2}s+1}\right) \tag{19}$$

Notice that the overall controller is similar to the classical (or interacting) PID form. The controller can be transformed into an ideal PID augmented with filter (i.e., PIDF controller):

$$G_C(s) = K_{Ca}\left(1+\frac{1}{\tau_{Ia}s}+\tau_{Da}s\right)\left(\frac{1}{\tau_f s+1}\right) \tag{20}$$

By comparing equations (19) and (20), the PIDF controller parameters are expressed as follows:

$$\begin{cases} K_{Ca} = \dfrac{K_{c1}K_{a2}(\tau_I+\tau_{m2})}{\tau_I} \\ \tau_{Ia} = \tau_I + \tau_{m2} \\ \tau_{Da} = \dfrac{\tau_I\tau_{m2}}{\tau_I+\tau_{m2}} \\ \tau_f = \tau_{c2} \end{cases} \tag{21}$$

2.3. MSC-RS Design Algorithm

Figure 2 shows the proposed Multi-Scale Control with Routh Stability (MSC-RS) design procedure using the equations derived in Section 2.2. The first step is to obtain the SOPDT model of the given process using the step test. Once the SOPDT model is available, the designer can apply the decomposition equations to determine two process modes. The next step (3) is vital because the designer has to specify values for the dimensionless tuning parameters (r_{p1}, r_{p2} and r_i). Considering the designer might have little idea of the appropriate tuning values, the known ranges of the dimensionless parameters can help - provided the values are within bounds and the closed-loop system should be stable. In this paper, the recommended values for r_{p1} and r_{p2} are 0.5 and 0.7, respectively. Given these parameter values, the designer can adjust the value of r_i accordingly to meet the design criteria. Initially, the designer can use $r_i = 2$.

The recommended design criteria: $8dB \le GM \le 10dB$, $55^o \le PM \le 65^o$, and $3\% \le OS \le 6\%$. Here, GM, PM, and OS correspond to the gain margin, phase margin, and percentage overshoot. Note that the designer can specify the design criteria appropriate to the specific process of interest. It is advisable to keep the default values of r_{p1} and r_{p2} but adjust only the r_i value until the attainment of all design criteria. If the GM is outside the specified bound, the designer can readjust the r_{p1} value while keeping the r_{p2} at its default value. Then, the designer can refine the r_i value until all criteria are met.

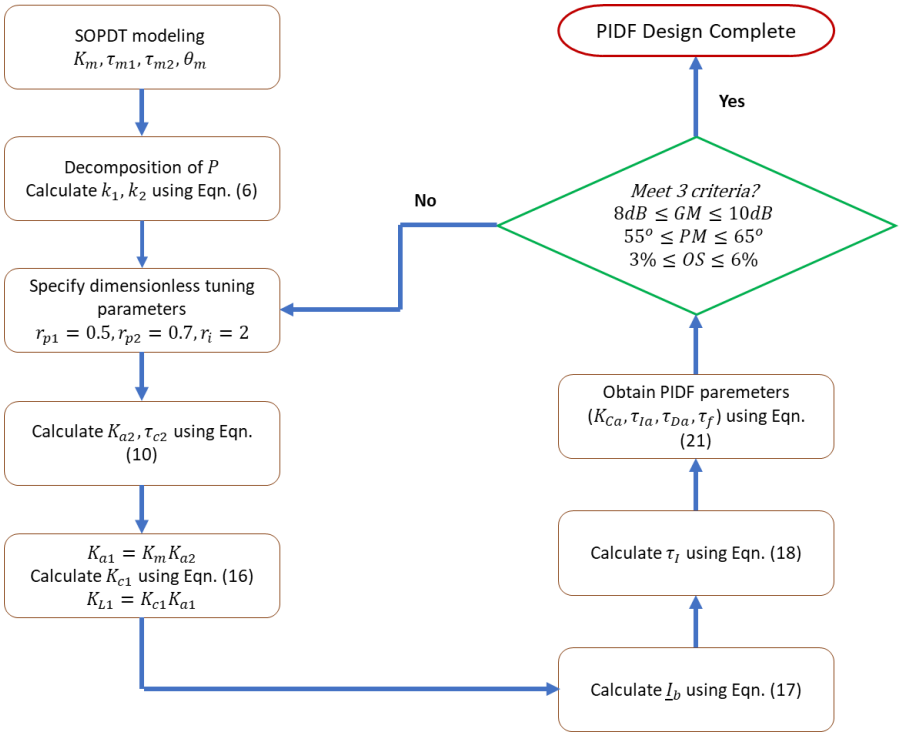

Figure 2. MSC-RS algorithm for designing a PIDF controller based on the SOPDT model.

3. Illustrative Example

To demonstrate the effectiveness of the MSC-RS design algorithm, we adopt the Coal Mill Temperature case study available in the Loop-Pro Trainer of Control Station (see https://controlstation.com/). The controlled variable is the coal mill temperature (T), the disturbance is the coal feed flow rate (D), and manipulated variable is the damper regulating fresh air flow (U). The nominal operating conditions are $U = 50\%$, $T = 90^oC$, and $D = 10\ tons/hr$. Applying a step test to the manipulated variable with a magnitude of 10% (i.e., step up from 50% to 60%) generates the required plant data for fitting the SOPDT model. The sampling period for data recording is 0.1 s. The Loop-Pro can curve fit the data into the desired model. Here, two model fittings are applicable: First-Order plus Deadtime (FOPDT) and SOPDT models. The FOPDT and SOPDT models are as below:

FOPDT

$$G_m(s) = \frac{-2.42\exp(-28.75s)}{52.71s + 1} \quad where\ R^2 = 0.9976 \tag{22}$$

SOPDT

$$G_m(s) = \frac{-2.28\exp(-17.59s)}{(28.78s + 1)(26.22s + 1)} \quad where\ R^2 = 0.9996 \tag{23}$$

In addition to designing a PIDF controller using the MSC-RS algorithm, we also obtain PIDF controllers using two well-known methods: SIMC and AMIGO step response available in the MATLAB™ Control System Designer (R2020a). Using each PIDF designer (i.e., AMIGO or SIMC), we obtain two PIDF controllers: one based on the FOPDT and another based on the SOPDT model. Note that the MSC-RS algorithm only gives one PIDF controller based on the SOPDT model, i.e., it does not apply to the FOPDT model. Table 1 shows the tuning, GM, and PM values of five PIDF controllers. For reference, the dimensionless parameter settings of the MSC-RS design are $r_{p1} = 0.5$, $r_{p2} = 0.7$ and $r_i = 1.6$.

The percentage overshoot (OS) assuming the deadtime is approximately representable using 1/1 Padě formula is $OS = 5\%$. Also note that the derivative action is based on the measured value, i.e., not based on the error. The measurement noise is assumed to have a six-sigma span of 0.3 (i.e., normally distributed noise).

Table 1. PIDF controller tuning values for the Coal Mill Temperature

Method	K_c $(\frac{^oC}{\%})$	T_I (min)	T_D (min)	T_f (min)	GM (dB)	PM (deg)
MSC-RS-SOPDT	-0.6984	54.36	13.57	0.22	9.7	59.8
AMIGO-FOPDT	-0.4390	47.00	13.30	1.20	10.3	61.1
SIMC-FOPDT	-0.4818	67.00	11.07	7.20	9.65	67.7
AMIGO-SOPDT	-0.4954	43.00	12.30	1.10	12.2	54.5
SIMC-SOPDT	-0.5581	64.00	10.56	6.30	9.52	60.5

Figure 3 shows the setpoint tracking responses under the PIDF controllers in Table 1 when the setpoint increases from 90^oC to 110^oC. Meanwhile, Table 2 shows the performance of the controllers based on the Integral Absolute error (IAE) values. Note that the PIDF controllers obtained using the SIMC and AMIGO methods, the PIDF controllers based on the FOPDT model demonstrate improved performances based on the IAE values. However, in term of the rise time, the PIDF tuned based on the SOPDT perform better than those based on the FOPDT. For the AMIGO method, the rise time corresponding to the PIDF based on the SOPDT is smaller, but its overshoot is higher than that based on the FOPDT. However, the overshoots shown by PIDF controllers obtained using the AMIGO and SIMC remain within acceptable bounds (between 3% and 13%), as advised in [4]. Therefore, the results suggest that using the more detailed SOPDT model for the PIDF controller tuning might not necessarily yield a controller with a better performance than the one based on the FOPDT model.

Another important conclusion is that the PIDF controller obtained using the MSC-RS substantially outperforms the other PIDF controllers, i.e., it has the shortest rise and settling time, and smallest IAE value. Also, its overshoot is relatively low compared to the overshoots displayed by other controllers. In other words, the PIDF controller obtained via the MSC-RS algorithm produces smooth and fast setpoint tracking. Therefore, this result shows that the MSC-RS algorithm has the potential to give enhanced setpoint performance over the AMIGO and SIMC methods based on the SOPDT model.

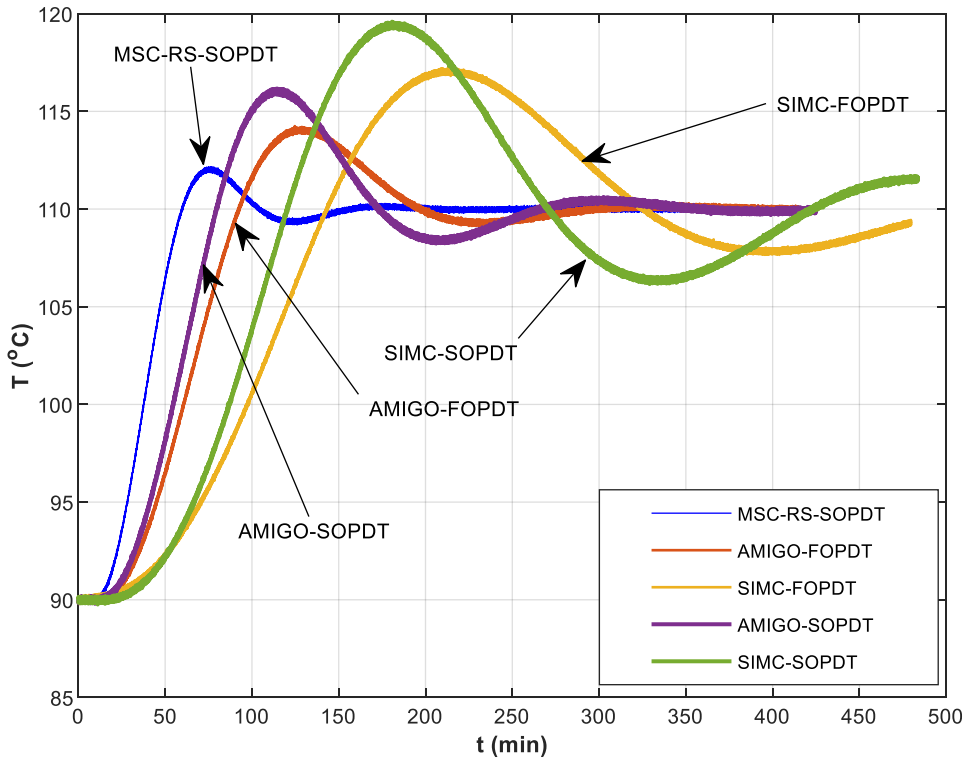

Figure 3. Setpoint tracking responses.

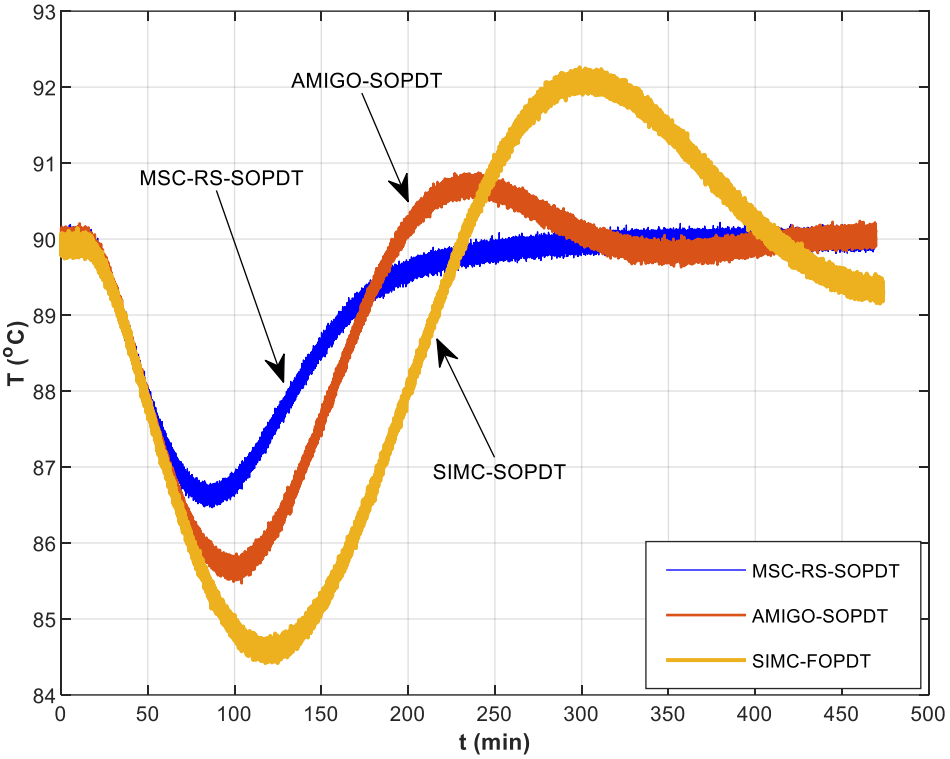

Figure 4. Disturbance rejection (step increase in coal feed from 10 ton/hr to 20 ton/hr (AMIGO and SIMC methods based on SOPDT model).

Next, Figure 4 displays the disturbance rejection performances when the coal feed flow rate increases from 10 $tons/hr$ to 20 $tons/hr$ while keeping the setpoint at 90^oC. Table 2 shows the IAE values corresponding to the five PIDF controllers. The disturbance rejection response of the PIDF controller obtained using the MSC-RS algorithm is substantially faster than the controllers obtained using the AMIGO or SIMC method in terms of the settling time (time to reach the zone of $\pm 5\%$ of the setpoint value. Also, the PIDF controller obtained via the MSC-RS algorithm gives the smallest IAE magnitude. The PIDF controller obtained using the SIMC shows the longest settling time and largest IAE value. Overall, the best disturbance rejection performance is by the MSC-RS's PIDF controller, followed by that of the AMIGO's PIDF, and the last one is by the SIMC's PIDF controller.

Table 2. Comparative performances of the PIDF controllers based on IAE values.

Method	Setpoint Tracking	Disturbance Rejection
MSC-RS-SOPDT	835.0	367.7
AMIGO-FOPDT	1490.7	565.0
SIMC-FOPDT	2891.5	1097.8
AMIGO-SOPDT	1526.9	504.7
SIMC-SOPDT	2961.8	952.9

4. Conclusions

The work has established a new tuning rule (i.e., MSC-RS algorithm) for designing the PIDF controller based on the SOPDT model. Demonstrating the new algorithm in designing a PID controller to control the Coal Mill temperature highlights two crucial results. First, the PIDF controller design based on the higher-order SOPDT model can lead to better performance than the simple FOPT model for the SIMC and AMIGO methods for the disturbance rejection case, and vice versa for the setpoint tracking. Second, the new MSC-RS algorithm can lead to a PIDF controller with improved performance (i.e., setpoint tracking or disturbance rejection) over that obtained using the well-known SIMC or AMIGO method. Furthermore, the MSC-RS algorithm is flexible in achieving desired performance

requirements by adjusting its three dimensionless tuning parameters (r_{p1}, r_{p2}, and r_i), which have well-established ranges to ensure closed-loop stability. Unlike the SIMC or AMIGO method, the MSC-RS has a higher degree of freedom (more adjustable parameters) for easy modification to the algorithm to achieve a wide range of desired criteria. Potential future research directions include extending the current approach to integrating/unstable SISO and MIMO systems.

Acknowledgments: The author would like to thank Curtin University Malaysia for providing facility to conduct this research.

References

1. J. Aoyama, K. Konishi, T. Yamamoto and T. Hinamoto, "A BMI based design for robust PID controllers with two-degrees-of-freedom structure.," in *Proceedings of the 2004 American Control Conference.*, 2004.
2. D. B. Ender, "Process control performance: Not as good as you think.," *Control Engineering,* vol. 40, no. 10, pp. 180-190, 1993.
3. A. O'dwyer, Handbook of PI and PID controller tuning rules., World Scientific, 2009.
4. R. P. Borase, D. K. Maghade, S. Y. Sondkar and S. N. Pawar, "A review of PID control, tuning methods and applications.," *International Journal of Dynamics and Control ,* vol. 9, pp. 818-827, 2021.
5. S. Skogestad, "Simple analytic rules for model reduction and PID controller tuning.," *Journal of Process control,* vol. 13, no. 4, pp. 291-309, 2003.
6. K. J. Astrom and T. Hagglund, "Revisiting the Ziegler-Nichols step response method for PID control.," *Journal of Process Control,* vol. 14, no. 6, pp. 635-650, 2004.
7. J. Nandong and Z. Zang, "High-performance multi-scale control scheme for stable, integrating and unstable time-delay processes.," *Journal of Process Control,* vol. 23, no. 10, pp. 1333-1343, 2013.
8. Q. H. Seer and J. Nandong, "Stabilization and PID tuning algorithms for second-order unstable processes with time-delays.," *ISA transactions,* vol. 67, pp. 233-245, 2017.
9. Q. H. Seer and J. Nandong, "Multi-scale control scheme: Stabilization of a class of fourth-order integrating-unstable systems.," *Journal of the Franklin Institute,* vol. 355, no. 1, pp. 141-163, 2018.
10. J. Nandong and Z. Zang, "Multi-loop design of multi-scale controllers for multivariable processes.," *Journal of Process Control,* vol. 24, no. 5, pp. 600-612, 2014